

Anomalous low-temperature specific heat around the metal-insulator transition in ordered double-perovskite alloys $\text{Sr}_2\text{Fe}(\text{Mo}_{1-y}\text{W}_y)\text{O}_6$ ($0 \leq y \leq 1$)

T. Okuda,^{1,2} K.-I. Kobayashi,² Y. Tomioka,² and Y. Tokura^{2,3}¹*Department of Nano-structures and Advanced Materials, Kagoshima University, Kagoshima 890-0065, Japan*²*Correlated Electron Research Center (CERC), National Institute of Advanced Industrial Science and Technology (AIST), Tsukuba 305-0046, Japan*³*Department of Applied Physics, University of Tokyo, Tokyo 113-8656, Japan*

(Received 19 May 2003; published 3 October 2003)

Low-temperature excitation has been investigated for polycrystals of ordered double-perovskite alloys $\text{Sr}_2\text{Fe}(\text{Mo}_{1-y}\text{W}_y)\text{O}_6$ ($0 \leq y \leq 1$) by specific-heat measurements. Critical enhancement of excess low-temperature specific heat with anomalous power law in its T dependence has been observed around the metal-insulator transition, $y_c \sim 0.8$. Such low-energy excitations originate in a random mixture of ferromagnet and antiferromagnet in the face-centered-cubic lattice of the magnetic Fe sites.

DOI: 10.1103/PhysRevB.68.144407

PACS number(s): 75.40.Cx

Metal-insulator (MI) transition of transition-metal oxides has been investigated for long, but is still one of the most attractive issues in the field of condensed-matter physics. This is because many intriguing phenomena occur around the transition, such as high-temperature superconductivity in cuprates and colossal magnetoresistance in manganites.¹ The MI transitions have been argued in terms of various concepts, e.g., Mott transition,² localization effect,³ and phase separation.⁴ To elucidate a nature of the transition, especially important are the investigations of anomalous properties around the MI transition. Here we chose ordered double perovskites $\text{Sr}_2\text{Fe}(\text{Mo}_{1-y}\text{W}_y)\text{O}_6$ ($0 \leq y \leq 1$),⁵ which are a system of a random mixture of ferromagnet (FM) and antiferromagnet (AFM), and investigated their thermal properties reflecting low-energy excitations to clarify a nature of percolating MI transition.

In ordered double perovskites with formula of $A_2B'B''\text{O}_6$ (where A is an alkaline-earth or rare-earth ion), the transition-metal sites are occupied alternately by different cations B' and B'' .⁵⁻⁸ In particular, Fe-based oxides ($B' = \text{Fe}$, $B'' = \text{Mo}$ or Re) have attracted much attention as a novel class of magnetoresistive oxides, since the low-field tunneling-type magnetoresistance effect, originated in half-metallic nature, was found in $\text{Sr}_2\text{FeMoO}_6$ (SFMO) at room temperature.^{7,8} Among these ordered double-perovskite systems, a solid-solution system $\text{Sr}_2\text{Fe}(\text{Mo}_{1-y}\text{W}_y)\text{O}_6$ ($0 \leq y \leq 1$) is one of the composition-control MI transition systems.^{5,9} The end compound SFMO is a ferromagnetic metal with $T_C = 419$ K,^{7,8} where Fe^{3+} ($S = 5/2$) and Mo^{5+} ($S = 1/2$) couple antiferromagnetically. In this compound, local spins of $S = 5/2$ are produced from $3d^5$ electrons of Fe^{3+} ions, while the conduction band is partially occupied by the $4d^1$ electrons of Mo^{5+} .⁷ Another end compound of Sr_2FeWO_6 (SFWO) is an antiferromagnetic insulator with $T_N = 37$ K,^{5,9} where Fe^{2+} ion is in the high-spin state ($S = 2$), and W^{6+} ion ($5d^0$) is in the nonmagnetic state. In such a solid-solution system, the ferromagnetic metal (FMM) to ferromagnetic insulator (FMI) transition is induced by substitution of Mo by W on the B'' site around $y_c \sim 0.8$, as shown in the Fig. 1. This MI transition occurs in a

percolating manner. In this site-selective (B'' -site) solid-solution system, the nominal valence states of Mo and W remain as $5+$ and $6+$, respectively, in the whole y region.⁵ One of the evidences for such a percolation process is the y dependence of the electronic specific-heat coefficient γ .⁵ γ decreases almost linearly with y in $0 \leq y < 0.8$, which comes from the volumetric ratio of the ferromagnetic metallic domains to the antiferromagnetic insulating domains below the critical concentration, $y_c \sim 0.8$. Such a behavior of γ value is quite different from those in the bandwidth-control FMM-FMI transition in the ordered double-perovskite systems such as $(\text{Sr}_{1-x}\text{Ca}_x)_2\text{FeReO}_6$.¹⁰ In this paper, we report the finding of large low-temperature entropy arising from low-energy excitations around the MI transition in $\text{Sr}_2\text{Fe}(\text{Mo}_{1-y}\text{W}_y)\text{O}_6$ ($0 \leq y \leq 1$) system.

To clarify the mechanism of MI transition, we have investigated the specific heat of $\text{Sr}_2\text{Fe}(\text{Mo}_{1-y}\text{W}_y)\text{O}_6$. The polycrystalline samples are prepared by solid-state reaction. The details of synthetic conditions as well as structural, chemical, transport, and magnetization characterizations of the obtained polycrystals have been reported previously.⁵ As described in Ref. 5, there is no structural phase transition in the whole y region. The samples show nearly perfect ordering of B' and B'' sites [Fe vs (Mo, W) sites] for $y \geq 0.2$, while random mixing of Mo and W in B'' site is maintained in the whole composition. The B -site ordering ratio of the $y = 0$ sample is about 0.91, which leads to the smaller saturation magnetization of about $3.5\mu_B/\text{f.u.}$ than the ideal full moment value ($4\mu_B/\text{f.u.}$). The specific heat of the polycrystals, which were from the same batches used in Ref. 5, were measured in ³He cryostat at the temperatures from 0.5 K to 100 K.

Figure 1 shows the temperature (T) dependence of resistivity ρ and magnetization M in $\text{Sr}_2\text{Fe}(\text{Mo}_{1-y}\text{W}_y)\text{O}_6$ polycrystals. The data in Fig. 1 are derived from Kobayashi *et al.* (Ref. 5). Except for $y = 1$ (Sr_2FeWO_6), all the samples are in a ferromagnetic state at low temperature. The FMM-FMI transition occurs around $y_c \sim 0.8$ with the increase of y . The M - T curve for $0.6 \leq y < 1$ polycrystals has broadened peak features around 50 K without a significant variation of

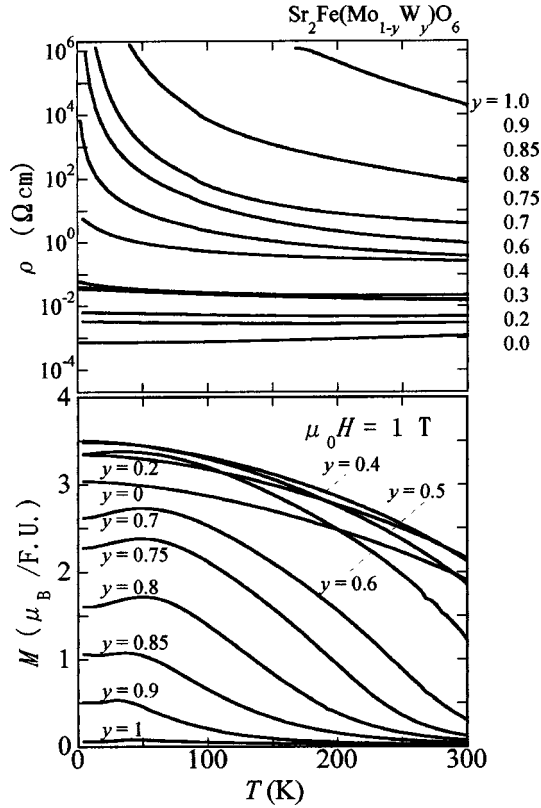


FIG. 1. T dependence of resistivity ρ and magnetization M in $\text{Sr}_2\text{Fe}(\text{Mo}_{1-y}\text{W}_y)\text{O}_6$ ($0 \leq y \leq 1$), after Kobayashi *et al.* (Ref. 5). The M - T curve for $0.6 \leq y < 1$ samples has broadened peak features around 50 K without a significant variation of peak temperatures.

peak temperature. In this region of y between 0.6 and 1, the long-range ferromagnetic correlations at low temperatures rapidly increase with the decrease of y from 1, as the FMM clusters gradually grow in the percolation manner in the insulating background with weak antiferromagnetism. Such growth of FMM clusters leads to anomalous low-energy magnetic excitations, as described in the following.

Figure 2(a) shows the T variation of the remanent specific heat ($C - \gamma T$) for the $y=0$ (SFMO), 0.8, and 1 (SFWO) samples, where γ is the electronic specific-heat coefficient that was evaluated from the C/T values extrapolated to 0 K.⁵ A sharp peak is clearly observed at $T_N = 37$ K in the curve of SFMO. This sharp peak is completely extinguished only by slight substitution of W with Mo, which contrasts the magnetization behavior with the subsisting broadened peak around 50 K. As shown in Fig. 2(a), there is no anomaly in the curve of the $y=0.8$ sample in the T region below 100 K. Alternatively, the extra specific heat appears at low temperatures, which is enhanced around the MI transition, $y_c \sim 0.8$. Gray solid lines in Fig. 2(a) are the calculated phonon contributions C_{latt} by using the Debye model as follows:

$$C_{latt} = 9rNk_B \left(\int_0^{\theta_B/T} \frac{x^3}{e^x - 1} dx - \frac{\theta_B/T}{e^{\theta_B/T} - 1} \right), \quad (1)$$

where θ_B is the Debye temperature. In this paper, θ_B of about 338 K was obtained for SFMO from the raw specific-

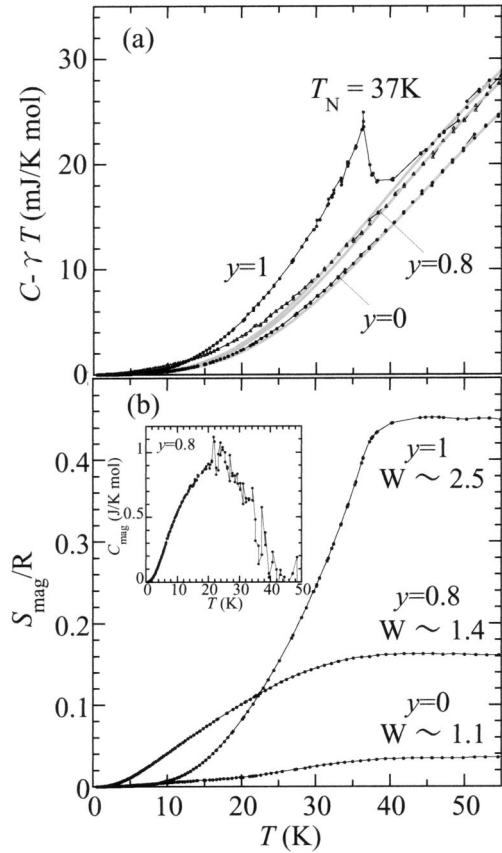


FIG. 2. (a) The curve of $C - \gamma T$ vs T , in which gray solid lines represent the calculated phonon contribution $C_{lattice}$ (see text) is shown. The term γT stands for the electronic contribution. (b) The curves of S_{mag} vs T , where S_{mag} is a remanent magnetic entropy (see text), are shown. The inset to (b) shows the magnetic component of the specific heat ($C_{mag} = C - \gamma T - C_{lattice}$). For $y=1$, the antiferromagnetic transition is manifested as the sharp peak at $T_N = 37$ K, while for the other compounds a peak does not appear at all in the specific-heat data.

heat data, in which we can separately estimate the electric and magnetic contributions to the specific-heat data.⁸ The θ_B values for other samples were estimated by using their density and the θ_B value of SFMO. The phonon contributions estimated without any adjustable parameter explain well the data above 50 K, where the contributions for other low-energy excitations can be neglected. In this plot, we can clearly see the enhancement of low- T specific heat below 20 K in the $y=0.8$ sample.

Figure 2(b) shows the T dependence of the estimated magnetic entropy [$S_{mag} = \int^T (C_{mag}/T) dT$], deduced by the subtraction of electronic and phonon contributions from the total one ($S_{mag} = S - S_{el} - S_{latt}$). For $y=1$ (SFWO), the magnetic entropy sharply decreases with the decrease of T below T_N . The variation of number of state (W) is estimated to be about 2.5, which is a half of the anticipated value, $2S + 1 = 5$. For $y=0.8$, S_{mag} gradually decreases around 40 K with decreasing T . As seen in the S_{mag} - T curve, a large remanence of magnetic entropy can be seen below 20 K, in contrast with the $y=0$ and $y=1$ samples.

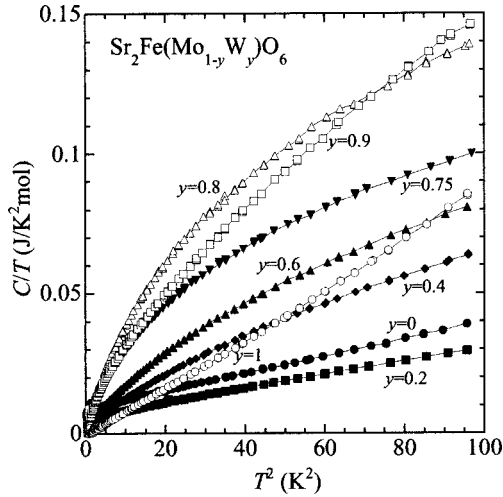


FIG. 3. Low-temperature specific heat below 10 K plotted as C/T vs T^2 for $y=0, 0.2, 0.4, 0.6, 0.75, 0.8, 0.9$, and 1.

To investigate the low-energy excitation in detail, we measured the low-temperature specific heat over the whole y region. Figure 3 plots the specific-heat data as C/T vs T^2 for $y=0, 0.2, 0.4, 0.6, 0.75, 0.8, 0.9$, and 1. One can immediately notice that the low-temperature specific heat is enhanced toward $y_c \sim 0.8$ with the increase of y and decreases with the further increase of y from y_c toward 1. Figure 4 (a) shows the y dependence of S_{mag} at 10 K. In this plot, S_{mag} is found to be critically enhanced around the MI transition. For $y=0$ (SFMO), S_{mag} is due to the excitation of ferromagnetic magnons, while for the $y=1$ sample (SFWO) it is due to the excitation of antiferromagnetic magnons. As compared with these magnon excitations of the two end compounds, the low-energy excitations around the MI transition seems to bear anomalously large entropy. The remanent specific heat C_r below 20 K, deduced by the subtraction of electric and phonon contributions from the total one, is fitted by the equation as follows:

$$C_r = C - C_{el} - C_{latt} = \alpha T^{1.5} + \nu T^\epsilon. \quad (2)$$

The first term on the right-hand side expresses the contribution from ferromagnetic magnons and the second term from extra thermal excitations. For $y=0$, $\nu \approx 0$ and for $y=1$, $\alpha \approx 0$ and $\epsilon \approx 3$, because the antiferromagnetic magnon contribution is proportional to T^3 . The obtained α and ϵ are shown in Figs. 4(a) and 4(b). The ordinary ferromagnetic magnon contribution is appreciable only in the low- y region as seen in the y variation of the α value. Note that the absolute value of magnetic entropy at 10 K in this regime is quite small, compared with the one in the y region around the MI transition. After the conventional ferromagnetic magnon excitation fades out, the unknown low-energy excitation is critically enhanced around the MI transition as seen in the y -variation of the S_{mag} value in Fig. 4(a). The power ϵ of T dependence of low-temperature specific heat also varies from 1.7 to 2.6 with the change of y . The ϵ value takes the minimum of ≈ 1.7 at $y=0.8$ [see the inset of Fig. 4(b)], where S_{mag} becomes maximum.

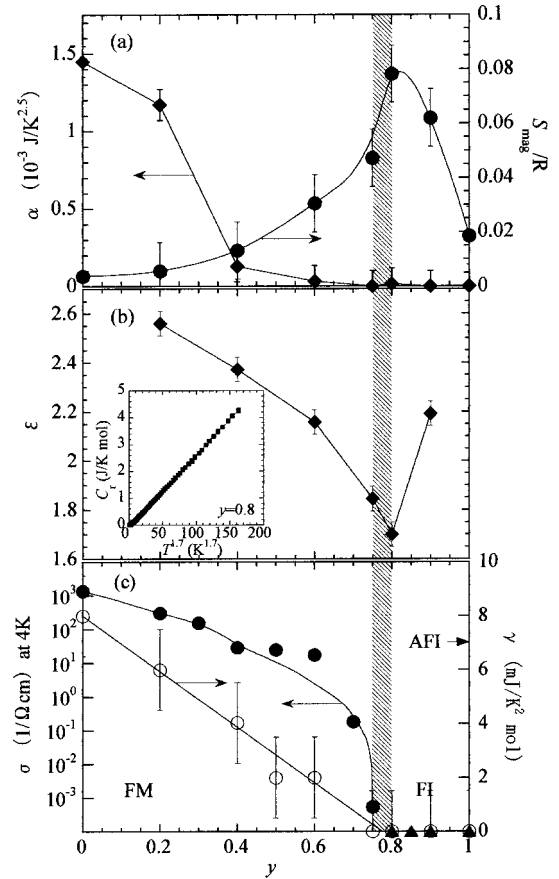


FIG. 4. The y dependence of (a) $T^{1.5}$ coefficient α of low-temperature specific heat and magnetic entropy below 10 K (S_{mag}), (b) power ϵ in the form of T^ϵ for extra specific heat below 20 K, and (c) conductivity σ and electronic specific-heat coefficient γ . σ in (c) is essentially zero for $y \geq 0.8$, represented by triangles. The α and ϵ values are deduced from fitting the remanent specific heat C_r by Eq. (2) (see text) and the γ and σ values in (c) are derived from Kobayashi *et al.* (Ref. 5). A hatched vertical bar indicates the MI phase boundary. The inset in (b) shows C_r of $y=0.8$ plotted against $T^{1.7}$.

Such a critical behavior cannot be explained by the mass-renormalization effect, which would give rise to the large- T linear specific heat, as observed in a canonical Mott transition system. As seen in Fig. 4(c) (the data of which are from Ref. 5), the γ values in this system appear to be proportional to $|y_c - y|$, implying that the metallic volume is changing with y while keeping the carrier effective mass constant. One of the possible scenarios to explain such a critical behavior is a ferromagnetic fracton model¹¹ in a percolating FM on a background of weak AFM. In an isotropic percolating magnet, a ferromagnetic fracton excitation was theoretically predicted.¹¹ In this model, the mechanism of spin-wave excitation varies with the relation between a percolating correlation length ξ and a wavelength λ of spin wave. When $\lambda \gg \xi$, a spin-wave excitation has the same dispersion relation as a Heisenberg ferromagnet, giving the $T^{1.5}$ dependence in the low-temperature specific heat. This situation seems to correspond to the feature in the low- y region below ~ 0.5 , where the $T^{1.5}$ dependence was observed [Fig. 4(a)]. When

$\lambda \ll \xi$, the short-wavelength excitation must propagate along the percolating pathway provided by the dilute arrangement of exchange-coupled spins. In this regime, the spin-wave stiffness decreases toward the percolation threshold and, therefore, the thermal magnetic excitation is much more enhanced. This behavior seems to be well consistent with the observed one qualitatively. According to the theoretical result,¹¹ however, the power in T dependence of low-temperature specific heat at the threshold is predicted to be below 1, which is smaller than the observed ϵ value of 1.7 at $y_c \sim 0.8$, as shown in Fig. 4(b). Furthermore, the power becomes larger with y departing from y_c . Such values are inconsistent with that predicted by a ferromagnetic fracton model in which ϵ must not exceed 1.5.

A more plausible model than the ferromagnetic fracton model is the reentrant spin-glass (RSG) model.¹² A random mixture of FM and AFM often gives rise to spin-glass (SG) order. Furthermore, it is possible to give rise to the state where a long-range ferromagnetic order and SG order coexist, if the randomness and frustration are rather weak. According to the mean-field theory of the random network model for FM-SG system,¹³ the competition between the SG and the FM can sometimes give a spatially segregated coexistence of the two systems in the low-temperature reentrant region.¹⁴ Such a segregation picture is consistent with our percolation scenario. In the present system, the random mixture of FM and weak AFM may also give the RSG state at low temperatures, including FM metallic region and SG insulating region. The cusp around 50 K of the M - T curve (in Fig. 1) may be recognized as a signal of such a RSG state, i.e., partial destruction of long-range FM order by the random-field effect of growing SG correlation with the decrease of T .¹⁵

The observed enhancement of low-temperature specific heat around the MI phase boundary may reflect the critical enhancement of degree of SG correlation around the percolation threshold y_c . With the decrease of y from 1 toward y_c , the FM cluster grows. Then the competition between the FM and the AFM order becomes stronger and the SG corre-

lation develops with increase of randomness and frustration. With the further decrease of y from y_c to 0, however, the connected FM networks grows, and the growing FM correlation suppresses the SG order. In other words, the long-range FM order produces an effective magnetic field working on spins of SG region. The increase of effective field and the decrease of volume fraction of SG region may suppress the low-energy magnetic excitation with decreasing y from y_c .¹² Such a broad peak, as generally observed in SG systems, is absent in the T dependence of specific heat in the whole y region. However this may be due to this effective magnetic field produced by the FM order, which may play the same role as an external magnetic field flattening the peak profile in the specific heat of SG.¹² A weak-peak profile of the deduced magnetic specific heat C_{mag} in the inset of Fig. 2 bears some analogy to a remanent peak profile under a magnetic field. The T dependence of specific heat may be also explained by the same model: It is widely known for ordinary SG systems that the low-temperature magnetic specific heat is proportional to T^α ($1 \leq \alpha \leq 2$) (Ref. 16) and the higher α values appear in a sufficiently high magnetic field.¹⁷

In summary, we have investigated the specific heat of the MI transition system, $\text{Sr}_2\text{Fe}(\text{Mo}_{1-y}\text{W}_y)\text{O}_6$ ($0 \leq y \leq 1$), and found anomalous enhancement of low-energy magnetic excitation around y_c . This low-energy excitation originates in a random mixture of ferromagnet ($\text{Sr}_2\text{FeMoO}_6$) and antiferromagnet (Sr_2FeWO_6) in the fcc lattice of spin-carrying Fe sites. The mixture perhaps gives rise to low-energy excitations characteristic of the reentrant spin glass rather than ferromagnetic fractons, although anomalous y -dependent power law in the T -dependence of low-temperature magnetic specific heat is still left to be quantitatively elucidated.

The authors would like to thank Y. Okimoto, H. Kato, Y. Motome, and K. Ohgushi for enlightening discussions. This work was supported in part by the New Energy and Industrial Technology Development Organization of Japan (NEDO), the Iwatani Naoji Foundation's Research Grant, and the Mazda Foundation's Research Grant.

¹M. Imada, A. Fujimori, and Y. Tokura, *Rev. Mod. Phys.* **70**, 1039 (1999).

²N.F. Mott, *Metal-Insulator Transitions* (Taylor and Francis, London, 1990).

³P.A. Lee and T.V. Ramakrishnan, *Rev. Mod. Phys.* **57**, 287 (1985); D. Belitz and T.R. Kirkpatrick, *ibid.* **66**, 261 (1994).

⁴A. Moreo, S. Yunoki, and E. Dagotto, *Science* **283**, 5410 (1999).

⁵K.-I. Kobayashi, T. Okuda, Y. Tomioka, T. Kimura, and Y. Tokura, *J. Magn. Mater.* **218**, 17 (2000).

⁶A.W. Sleight and J.F. Weither, *J. Phys. Chem. Solids* **33**, 679 (1972).

⁷K.-I. Kobayashi, T. Kimura, H. Sawada, K. Terakura, and Y. Tokura, *Nature (London)* **395**, 677 (1998).

⁸Y. Tomioka, T. Okuda, Y. Okimoto, R. Kumai, K.-I. Kobayashi, and Y. Tokura, *Phys. Rev. B* **61**, 422 (2000).

⁹T. Nakagawa, K. Yoshikawa, and S. Momura, *J. Phys. Soc. Jpn.* **27**, 880 (1969).

¹⁰H. Kato, T. Okuda, Y. Okimoto, Y. Tomioka, K. Oikawa, T. Kamiyama, and Y. Tokura, *Phys. Rev. B* **65**, 144404 (2002).

¹¹T. Nakayama and K. Yakubo, *Rev. Mod. Phys.* **66**, 381 (1994).

¹²K. Binder and A.P. Young, *Rev. Mod. Phys.* **58**, 801 (1986).

¹³H. Takayama, *J. Phys. Soc. Jpn.* **61**, 2512 (1992).

¹⁴G. Aeppli, S.M. Shapiro, R.J. Birgeneau, and H.S. Chen, *Phys. Rev. B* **28**, 5160 (1983); **29**, 2589 (1984).

¹⁵Recently, similar reductions of dc and ac magnetic susceptibilities were observed at low temperatures in ALaMnMoO_6 ($A = \text{Ba, Sr}$), in which the magnetic frustration occurred, due to the competition of two types of superexchange magnetic interactions; ferrimagnetic interactions between Mn and nearest-neighbor Mo ions and antiferromagnetic interactions between next-nearest-

neighbor Mn ions. [E.N. Caspi, J.D. Jorgensen, M.V. Lobanov, and M. Greenblatt, Phys. Rev. B **67**, 134431 (2003).] The paper concluded that a possibility of spin glass was ruled out in their cases because of the absence of frequency dependence of ac susceptibilities.

¹⁶L.R. Walker and R.E. Walstedt, Phys. Rev. Lett. **38**, 514 (1977); R. Caudron, P. Costa, J.C. Lasjaunias, and B. Levesque, J. Phys.

F: Met. Phys. **11**, 451 (1981); S. Süllou, G.J. Nieuwenhuys, A.A. Menovsky, J.A. Mydosh, S.A.M. Mentink, T.E. Masux, and W.J.L. Buyars, Phys. Rev. Lett. **78**, 354 (1997); J.A. Mydosh, *Spin Glasses: An Experimental Introduction* (Taylor and Francis, London, 1993).

¹⁷H. Akbarzadeh, P.H. Keeson, M.W. Meisel, and W.P. Halperin, Phys. Rev. B **29**, 2622 (1984).